Open Access

Catalysis Research

LIDSEN Publishing Inc.

Original Research

Spectrophotometric and Spectrofluorimetric Quantification of Urea via Silver Nanoparticles Prepared by Wet Chemical Method

Muhammad Ismail *

School of Environmental Science and Engineering, North China Electric Power University, 102206, Beijing, China; E-Mail: mismailchem@gmail.com

* **Correspondence:** Muhammad Ismail; E-Mail: mismailchem@gmail.com

Academic Editor: Narendra Kumar

Special Issue: Nanoparticles and Nanotechnologies in Catalysis

Catalysis Research
2023, volume 3, issue 1
doi:10.21926/cr.2301014

Received: November 09, 2022
Accepted: February 28, 2023
Published: March 15, 2023

Abstract

Silver nanoparticles have been utilized in an easy, sensitive, and effective approach through spectrophotometry and spectrofluorimetry to quantify urea in water samples. Here, 1,3-di-(1H-imidazole-1-yl) -2-propanol (DIPO) was employed to stabilize Ag NPs produced from the reduction of aqueous silver nitrate by sodium borohydride ($NaBH_4$). Beer-Lambert's law was applied for determination using the complexation of Ag NPs with urea molecules. The results show urea can be assessed concurrently with good results and percent recoveries. The UV-visible absorbance and fluorescence emission calibration curves were plotted at 445 and 471 nm wavelengths, respectively. Beer-Lambert's law was obeyed in the 0.1-15 mM concentration range. A linear correlation for both UV-visible spectrophotometry and spectrofluorimetry was obtained on optimum conditions using the suggested methods having a limit of detection (LOD) was found to be 0.897 and 0.048, respectively. The percent recovery ± RSD by the spectrophotometric and spectrofluorimetric method was found to be 88 ± 19.7%, 96.67 ± 21.53%, 130.8 ± 1.33% and 102.3 ± 12.7%, 97.26 ± 5.63%, 111.4 ± 3.8%, respectively. Following a comparison of the obtained data, it may be possible to identify spectroscopic approaches with greater efficacy and efficiency that may be used to determine urea's presence in actual samples of biological and non-biological fluids.

Keywords
Silver nanoparticles; urea; spectrophotometry; spectrofluorimetry

1. Introduction

Nanotechnology is concerned with synthesizing, characterizing, and using diverse materials by regulating the form and size of dimensions less than 100 nanometers [1-3]. Many researchers have been drawn to the development of ecologically benign methods for the synthesis of metallic nanoparticles, particularly silver, which has a wide range of applications in textiles, electronics, the environment, and the medicinal sectors [4-6]. Ag NPs are made by reducing silver salt using a variety of processes, including chemical, biogenic, photo-reduction, thermal and radiation [7-10]. These silver nanomaterials are used as a research tool in various sectors, like photodegradation of environmental pollutants, photocatalysts for removing hazardous substances, especially dyes, gases and biomedical wastes, cancer cells treatment and removal of heavy metals from water bodies [11-15]. Moreover, Ag NPs are utilized in biosensing to assess several chemical substances in environmental, laboratorial, and clinical serums [16-18]. Due to their cheapness, low operating time, and sensitivity, spectrometric methods for quantifying pharmaceuticals, heavy metal ions, urea, etc., are now being researched [19-21]. Urea makes up between 80 and 90 percent of the nitrogen excreted by humans [22-25]. On the other side, if the body cannot get rid of it, it might cause serious health issues including uremic syndrome or azotemia [26-29]. Because of its importance, researchers have paid close attention to urea analysis; it supports disease detection, controls biological processes, and facilitates the delivery of medications and formulations [30-33].

In this work, silver nanoparticles were prepared by reducing the salt of silver nitrate solution with sodium borohydride stabilized by DIPO. The produced silver nanoparticles were then used to detect urea by complexation utilizing a much simpler, quick, and more reliable approach that included spectrophotometry and spectrofluorimetry along with accuracy and precision. This study aims to efficiently and reliably apply the silver nanoparticles for quantifying urea in two spectrometric ways to find a better detection method in the scientific and medical sectors.

2. Experimental

2.1 Apparatus

All stirring was done on the Sh-4 model ceramic magnetic stirrer using cylindrical magnetic stirring bars. All absorbance measurements were performed on a UV-1602 UV-visible spectrophotometer (photodiode array) using a quartz cuvette with an optical path of 1 cm. All fluorescence measurements were obtained on a spectrofluorimeter (Perkin-Elmer LS55). SEM images of the prepared silver nanoparticles were acquired on SEM JEOL (JSM-5910, 20 kV). X-ray diffractometer acquired XRD pattern (adv. Bruker-D8, Cu Kα, 1.5418 Å).

2.2 Reagents

All reagents were of analytical grade and were not purified further. Throughout our investigation, deionized water was used to make all the solutions. Solutions prepared are: 1 mM silver nitrate $AgNO_3$ (Merck) solution, 1 mM DIPO solution (synthesized by Gero's method [34]), 1 mM sodium borohydride $NaBH_4$ (Merck), 1 mM Urea (Agrium) solution, dilute 1% HCl and NaOH (Merck) solution.

2.3 Preparation of Silver Nanoparticles

10 mL $AgNO_3$ (1 mM) solution was stirred for 15 minutes on a magnetic stirrer along 10 mL DIPO (1 mM) solution, followed by the addition of 0.5 mL $NaBH_4$ solution was dropped and stirred again for 15 more minutes, which led to Ag NPs conversion of whole solution from transparent to yellowish color that gives an initial indication of Ag NPs being prepared. The as-prepared silver nanoparticles were scanned on a UV-visible spectrophotometer in the 300-800 nm range and a spectrofluorimeter in the range of 250-650 nm with a 435 nm excitation wavelength. The schematic preparation of silver nanoparticles is illustrated in Scheme 1.

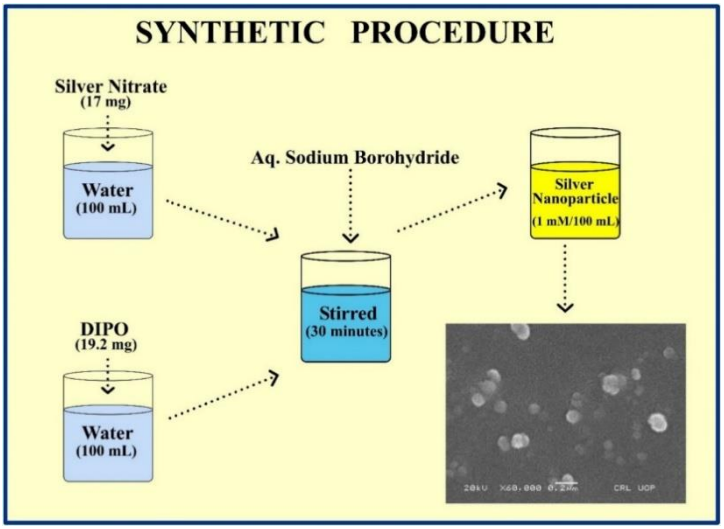

Scheme 1 Schematic presentation of synthetic procedure of Ag NPs.

2.4 Preparation of Ag NP-urea Complex

Firstly, prepared silver nanoparticles were used as a blank to record their UV-vis. Absorbance and fluorescence emission spectra have 300-800 nm and 250-650 nm with a 435 nm excitation wavelength, respectively. After that, 10 mL of prepared silver nanoparticles were combined with 10 mL urea (1 mM) solution, stirred for 15 minutes and the complex absorbance and fluorescence spectra were recorded.

2.5 Determination of Urea

Urea concentrations of 0.1-15 mM were mixed with prepared Ag NPs in a ratio of 10:1 (nanoparticle: urea). An absorbance and emission spectra at 435 nm were recorded and a regression equation was applied to both methods to calculate the concentration of urea once the calibration

curves were formed. Recovery experiments were conducted following the addition of a known quantity of pure urea to the different pre-analyzed urea concentration formulations to accurately and precisely analyze the suggested approach. Followed by the determination of the limit of detection (LOD), the limit of quantification (LOQ), the percent recovery, the standard deviation (SD) and the relative standard deviation (RSD).

3. Results and Discussion

3.1 Confirmation of Ag NPs Synthesis

The conversion of a solution containing silver nitrate and DIPO to dark yellow after adding $NaBH_4$ indicated the formation of Ag NPs. This was confirmed by the UV-vis spectrum showing an absorbance band at 406 nm, as seen in Figure 1 (a). This peak is, because of the metallic silver nanoparticles surface plasmon resonance (SPR) effect that verifies the Ag NPs formation. Additionally, spectrofluorimetric confirmation was performed at an excitation wavelength of 406 nm, showing emission spectra at 471 nm, as shown in Figure 1 (b).

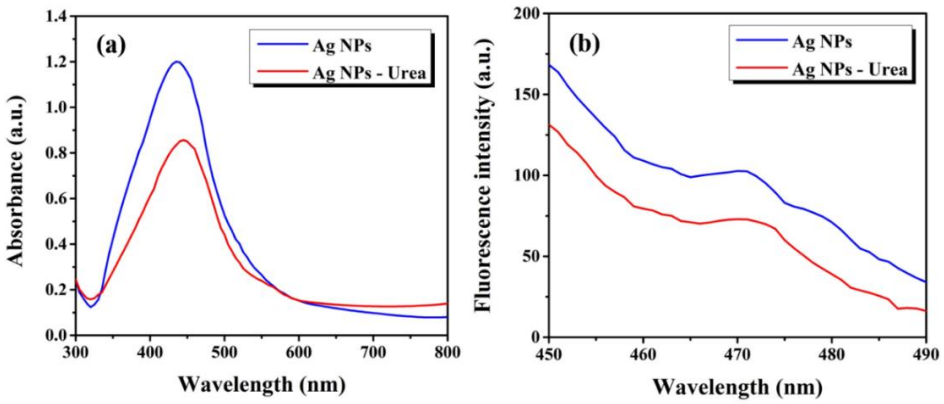

Figure 1 UV–Visible absorbance (a) and Fluorescence emission (b) spectra of Ag NPs.

3.2 Morphology Analysis of Ag NPs

SEM was used to examine the surface morphology and particle size of the as-prepared Ag NPs. Figures 2 (a) and Figure 2 (b) show Ag NPs as randomly dispersed particles having rough surfaces with irregular shapes. ImageJ software was used to determine the nanoparticle size, which was between 27 and 39 nm in size, with an average size of 32.9 nm.

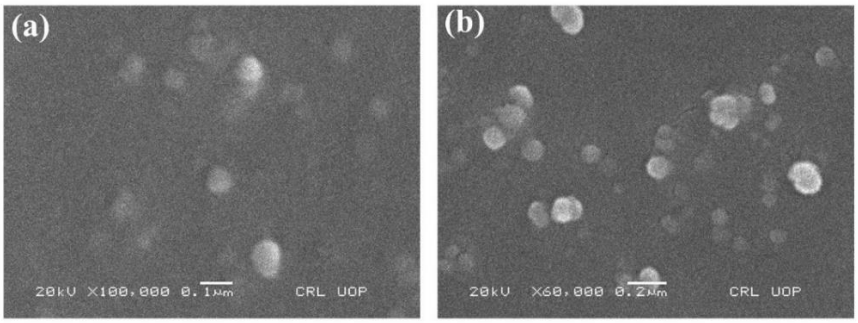

Figure 2 SEM images of Ag NPs (a and b).

Furthermore, the confirmation and phase purity of the prepared Ag NPs was analyzed by XRD; the result is depicted in Figure 3. The XRD pattern is matching with the powder diffraction file (# 04-0783) with lattice planes at 2 theta values of 38, 44, 64 and 74° indicating diffraction peaks (111), (200), (220) and (311), respectively. The XRD pattern showed no impurities, supporting the effective formation of Ag NPs.

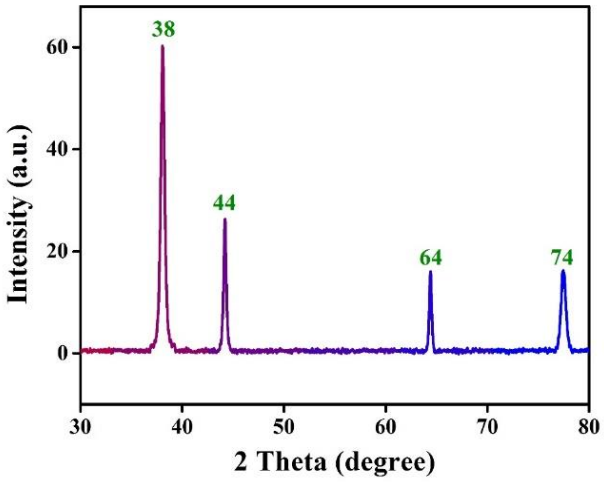

Figure 3 XRD pattern of prepared Ag NPs.

3.3 Complexation of Prepared Ag NPs with Urea

The formation of a complex between silver nanoparticles and urea was confirmed through UV-visible and spectrofluorimetric emission spectrum. Figure 1 (a) illustrates an absorption spectrum showing a red shift from 435 to 450 nm. This may be due to the complex formation between silver nanoparticles and urea. Besides, Figure 1 (b) displays an emission spectrum, showing a quenching of Ag NPs due to urea molecules from 450 to 490 nm. This may result from the new, non-fluorescent ground state (Ag NPs-urea complex) that absorbs radiation and returns within less time to the ground state without photon emission, which leads to quenching of emission spectra.

3.4 Determination of Urea

The urea concentration was quantified from both methods by Beer's-Lambert law. The maximum absorbance wavelength of 445 nm and fluorescence emission wavelength of 471 nm was chosen for plotting the calibration curves.

A linear correlation was obtained between absorbance/emission and urea concentration at the optimum conditions. Beer's law was obeyed in the 0.1-15 mM concentration range.

The spectrophotometric method calibration curve was plotted as shown in Figure 4 (a) obtaining slope 0.0065, intercept 0.0078 and correlation coefficient 0.96. SD, RSD, LOD, and LOQ from the calibration curve were calculated as 0.27 mM, 36.18%, 0.89 mM, and 2.72 mM respectively.

Similarly, a standard calibration curve was drawn for the spectrofluorimetric method from the urea concentration against the emission followed by applying the linear regression equations as shown in Figure 4 (b). The calibration curve shows slope 0.0073, correlation coefficient 0.99, SD 0.02 mM, RSD 9.60%, LOD 0.04 mM and LOQ 0.16 mM.

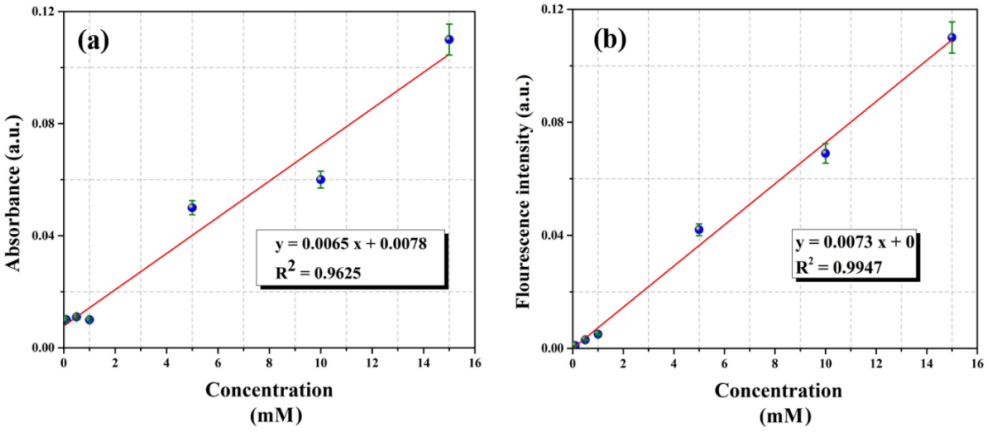

Figure 4 Calibration curve of Ag NPs by (a) UV-visible (b) Fluorescence.

Table 1 provides the summarized results for the urea determination. The results demonstrated that the suggested method may be used to determine urea satisfactorily.

Table 1 Analytical parameters for the determination of urea by Ag NPs.

Parameters	UV-Visible	Fluorescence
λmax (nm)	435	445
Linear range (mM)	0.1-15	0.1-15
LOD (mM)	0.89	0.04
LOQ (mM)	2.72	0.16
Correlation coefficient (R^2)	0.96	0.99
Regression equation	Y = 0.0065x + 0.0078	0.0073x
Slope	0.0065	0.0073
Intercept	0.0078	0
SD (mM)	0.27	0.02
RSD (%)	36.18	9.60

For analysis of recovery studies, the same sample of 0.5, 1, and 5 mM were tested three times each. The SD and RSD values were used to calculate the method's precision. The method's accuracy is demonstrated by the low SD and RSD results. % Recovery and RSD found by the spectrophotometric method shows 88.00 ± 19.7%, 96.67 ± 21.5%, and 130.80 ± 1.3%, respectively Table 2). Similarly, Table 3 demonstrates the % Recovery and RSD found by the spectrofluorimetric method, showing 102.30 ± 12.7%, 97.26 ± 5.6% and 111.40 ± 3.8%, respectively. The RSD values from both methods were satisfactory, indicating improved reproducibility of the suggested approaches. However, the spectrofluorimetric method shows good percent recovery with a small RSD suggesting high accuracy for determining urea.

Table 2 Precision and accuracy for spectrophotometric determination of urea.

S.No	Taken (mM)	Found (mM)	% Recovery	Average % Recovery ± RSD
1	0.5	0.34	67.60	88.00 ± 19.7%

2	0.5	0.49	98.40	
3	0.5	0.49	99.40	
4	1.0	0.90	90.00	
5	1.0	1.20	120.00	96.67 ± 21.5%
6	1.0	0.80	80.00	
7	5.0	6.64	132.80	
8	5.0	6.49	129.80	130.80 ± 1.3%
9	5.0	6.49	129.80	
			Total	86.00 ± 14.0%

Table 3 Precision and accuracy for spectrofluorimetric determination of urea.

S.No	Taken (mM)	Found (mM)	% Recovery	% Recovery ± RSD
1	0.5	0.44	87.67	
2	0.5	0.56	112.33	102.30 ± 12.7%
3	0.5	0.53	106.85	
4	1.0	1.03	102.74	
5	1.0	0.92	91.78	97.26 ± 5.6%
6	1.0	0.97	97.26	
7	5.0	5.75	117.00	
8	5.0	5.34	109.00	111.40 ± 3.8%
9	5.0	5.62	115.00	
			Total	103.65 ± 7.3%

4. Conclusion

The current work on silver nanoparticle synthesis is easy and inexpensive, and its function in urea determination is highlighted by simple, selective, sensitive, and low-cost approaches. The prepared silver nanoparticles were successfully employed to determine urea in pure samples using spectrophotometric and spectrofluorimetric methods, yielding good results. Both results revealed that the proposed methods for urea determination might be used successfully. From both methods, good RSD values were found, indicating improved repeatability. The suggested technique for determining urea is highly accurate since it has a high percent recovery and minimal RSD. Urea determination by spectrofluorimetric method shows a good result compared to the UV-visible method showing a good % recovery and less RSD, as shown in Table 4. Besides, our results have been compared with the previously reported methods, as shown in Table 5. From the table, it can be seen that the detection limit and LOD from our work are least as compared to other values previously reported having, the smaller value was found through the spectrofluorimetric method as compared to spectrophotometry. These techniques can be developed further and applied in further study for application in general and industrial analysis.

Table 4 Comparative results between proposed methods.

Method	% Recovery ± RSD	Average % Recovery ± RSD
Spectrophotometric	88.00 ± 19.7% 96.67 ± 21.5% 130.80 ± 1.3%	86.00 ± 14.0%
Spectrofluorimetric	102.30 ± 12.7% 97.26 ± 5.6% 111.40 ± 3.8%	103.65 ± 7.3%

Table 5 Comparison table for proposed and previously reported methods.

Material	Method	Linear range (mM)	Detection Limit (mM)	Reference
Diacetyl monoxime with Strong acids	Colorimetric	1.0–5.0	0.44	[35]
Electrostatic adsorption, carboxylic poly (vinyl chloride)	Potentiometric	0.01–100	0.28	[36]
Entrapment, poly (N-vinyl carbazole/stearic acid) Langmuir–Blodgett film	Potentiometric	0.5–68	0.50	[37]
Physical adsorption, electropolymerized toluidine blue film deposited on glassy carbon electrode	Amperometric	0.2–0.8	0.20	[38]
Encapsulation, biocomposite nonwoven nanofibre mat	Potentiometric	0.5–2.5	5.00	[39]
Microencapsulation, polymeric coating	Potentiometric	0.2–20	0.20	[40]
Ag NPs/DIPO/$NaBH_4$	Spectrophotometric	0.1–15	0.89	Present
Ag NPs/DIPO/$NaBH_4$	Spectrofluorimetric	0.1–15	0.04	Present

Acknowledgments

The authors are grateful to North China Electric Power University's (College of Energy Dynamics and Mechanical Engineering) in Beijing, China, for its assistance and supporting this work.

Author Contributions

The author confirms sole responsibility for the study conception, design, data collection, analysis, interpretation of results, and manuscript preparation.

Funding

The project did not receive any funding.

Competing Interests

The author declares no conflict of interests.

References

1. Purohit R, Mittal A, Dalela S, Warudkar V, Purohit K, Purohit S. Social, environmental and ethical impacts of nanotechnology. Mater Today Proc. 2017; 4: 5461-5467.
2. Bajpai VK, Kamle M, Shukla S, Mahato DK, Chandra P, Hwang SK, et al. Prospects of using nanotechnology for food preservation, safety, and security. J Food Drug Anal. 2018; 26: 1201-1214.
3. Krishna VD, Wu K, Su D, Cheeran MC, Wang JP, Perez A. Nanotechnology: Review of concepts and potential application of sensing platforms in food safety. Food Microbiol. 2018; 75: 47-54.
4. Dacoba TG, Olivera A, Torres D, Crecente-Campo J, Alonso MJ. Modulating the immune system through nanotechnology. Semin Immunol. 2017; 34: 78-102.
5. AlKahtani RN. The implications and applications of nanotechnology in dentistry: A review. Saudi Dent J. 2018; 30: 107-116.
6. Alaghaz AN, Zayed ME, Alharbi SA, Ammar RA, Chinnathambi A. Synthesis, spectroscopic identification, thermal, potentiometric and antibacterial activity studies of 4-amino-5-mercapto-S-triazole Schiff's base complexes. J Mol Struct. 2015; 1087: 60-67.
7. Shetti NP, Malode SJ, Nayak DS, Aminabhavi TM, Reddy KR. Nanostructured silver doped TiO_2/CNTs hybrid as an efficient electrochemical sensor for detection of anti-inflammatory drug, cetirizine. Microchem J. 2019; 150: 104124.
8. Shetti NP, Nayak DS, Malode SJ, Reddy KR, Shukla SS, Aminabhavi TM. Electrochemical behavior of flufenamic acid at amberlite XAD-4 resin and silver-doped titanium dioxide/amberlite XAD-4 resin modified carbon electrodes. Colloids Surf B. 2019; 177: 407-415.
9. Shikandar DB, Shetti NP, Kulkarni RM, Kulkarni SD. Silver-doped titania modified carbon electrode for electrochemical studies of furantril. ECS J Solid State Sci Technol. 2018; 7: Q3215.
10. Khan SA, Jain M, Pandey A, Pant KK, Ziora ZM, Blaskovich MA, et al. Leveraging the potential of silver nanoparticles-based materials towards sustainable water treatment. J Environ Manage. 2022; 319: 115675.
11. Padervand M, Asgarpour F, Akbari A, Eftekhari Sis B, Lammel G. Hexagonal core–shell SiO_2[–MOYI] Cl–]Ag nanoframeworks for efficient photodegradation of the environmental pollutants and pathogenic bacteria. J Inorg Organomet Polym Mater. 2019; 29: 1314-1323.
12. Padervand M, Ghasemi S, Hajiahmadi S, Rhimi B, Nejad ZG, Karima S, et al. Multifunctional Ag/AgCl/$ZnTiO_3$ structures as highly efficient photocatalysts for the removal of nitrophenols, CO_2 photoreduction, biomedical waste treatment, and bacteria inactivation. Appl Catal A Gen. 2022; 643: 118794.
13. Padervand M, Rhimi B, Wang C. One-pot synthesis of novel ternary $Fe_3N/Fe_2O_3/C_3N_4$ photocatalyst for efficient removal of rhodamine B and CO_2 reduction. J Alloys Compd. 2021; 852: 156955.

14. Xin Y, Zhu Q, Gao T, Li X, Zhang W, Wang H, et al. Photocatalytic NO removal over defective Bi/BiOBr nanoflowers: The inhibition of toxic NO_2 intermediate via high humidity. Appl Catal B. 2023; 324: 122238.
15. Padervand M, Hajiahmadi S. Ag/AgCl@ Tubular g-C_3N_4 nanostructure as an enhanced visible light photocatalyst for the removal of organic dye compounds and biomedical waste under visible light. J Photochem Photobiol A. 2022; 425: 113700.
16. Padervand M, Nasiri F, Hajiahmadi S, Bargahi A, Esmaeili S, Amini M, et al. Ag@Ag_2MoO_4 decorated polyoxomolybdate/C_3N_4 nanostructures as highly efficient photocatalysts for the wastewater treatment and cancer cells killing under visible light. Inorg Chem Commun. 2022; 141: 109500.
17. Padervand M, Heidarpour H, Goshadehzehn M, Hajiahmadi S. Photocatalytic degradation of 3-methyl-4-nitrophenol over Ag/AgCl-decorated/[MOYI]-coated/ZnO nanostructures: Material characterization, photocatalytic performance, and in-vivo toxicity assessment of the photoproducts. Environ Technol Innov. 2021; 21: 101212.
18. Padervand M. Reusable porous Na(SiAl)O_6.xH_2O/$NiFe_2O_4$ structure for selective removal of heavy metals from waste waters. Alexandria, VA: United States Patent; 2021; Patent No.: US 11,014,082 B2.
19. Mihindukulasuriya SD, Lim LT. Nanotechnology development in food packaging: A review. Trends Food Sci Technol. 2014; 40: 149-167.
20. Nduom EK, Bouras A, Kaluzova M, Hadjipanayis CG. Nanotechnology applications for glioblastoma. Neurosurg Clin. 2012; 23: 439-449.
21. Sozer N, Kokini JL. Nanotechnology and its applications in the food sector. Trends Biotechnol. 2009; 27: 82-89.
22. Gallocchio F, Belluco S, Ricci A. Nanotechnology and food: Brief overview of the current scenario. Procedia Food Sci. 2015; 5: 85-88.
23. Levy-Nissenbaum E, Radovic-Moreno AF, Wang AZ, Langer R, Farokhzad OC. Nanotechnology and aptamers: Applications in drug delivery. Trends Biotechnol. 2008; 26: 442-449.
24. Liu X, Wang D, Li Y. Synthesis and catalytic properties of bimetallic nanomaterials with various architectures. Nano Today. 2012; 7: 448-466.
25. Chandra J, Kandpal D, Gupta BR. Deals with thermo-elastic properties of nano-materials under high temperature. Phys B Condens Matter. 2009; 404: 1087-1109.
26. Yang H, Tao Q, Zhang X, Tang A, Ouyang J. Solid-state synthesis and electrochemical property of SnO_2/NiO nanomaterials. J Alloys Compd. 2008; 459: 98-102.
27. Wu R, Zhou K, Yue CY, Wei J, Pan Y. Recent progress in synthesis, properties and potential applications of SiC nanomaterials. Prog Mater Sci. 2015; 72: 1-60.
28. Shinke K, Ando K, Koyama T, Takai T, Nakaji S, Ogino T. Properties of various carbon nanomaterial surfaces in bilirubin adsorption. Colloids Surf B. 2010; 77: 18-21.
29. Cuenya BR. Synthesis and catalytic properties of metal nanoparticles: Size, shape, support, composition, and oxidation state effects. Thin Solid Films. 2010; 518: 3127-3150.
30. Gaddam RR, Kantheti S, Narayan R, Raju KV. Recent developments of camphor based carbon nanomaterial: Their latent applications and future prospects. Nano Struct Nano Objects. 2015; 3: 1-8.
31. Vorup-Jensen T, Boesen T. Protein ultrastructure and the nanoscience of complement activation. Adv Drug Deliv Rev. 2011; 63: 1008-1019.

32. Suh WH, Suslick KS, Stucky GD, Suh YH. Nanotechnology, nanotoxicology, and neuroscience. Prog Neurobiol. 2009; 87: 133-170.
33. Sanchez F, Sobolev K. Nanotechnology in concrete–A review. Constr Build Mater. 2010; 24: 2060-2071.
34. Gero A. Regularities in the basicity of some tertiary ethylenediamines, trimethylenediamines and 2-hydroxytrimethylenediamines. J Am Chem Soc. 1954; 76: 5158-5159.
35. Langenfeld NJ, Payne LE, Bugbee B. Colorimetric determination of urea using diacetyl monoxime with strong acids. PloS One. 2021; 16: e0259760.
36. Wu Z, Guan L, Shen G, Yu R. Renewable urea sensor based on a self-assembled polyelectrolyte layer. Analyst. 2002; 127: 391-395.
37. Singhal R, Gambhir A, Pandey MK, Annapoorni S, Malhotra BD. Immobilization of urease on poly (N-vinyl carbazole)/stearic acid Langmuir–Blodgett films for application to urea biosensor. Biosens Bioelectron. 2002; 17: 697-703.
38. Vostiar I, Tkac J, Sturdik E, Gemeiner P. Amperometric urea biosensor based on urease and electropolymerized toluidine blue dye as a pH-sensitive redox probe. Bioelectrochemistry. 2002; 56: 113-115.
39. Sawicka K, Gouma P, Simon S. Electrospun biocomposite nanofibers for urea biosensing. Sens Actuators B Chem. 2005; 108: 585-588.
40. Ternovskiĭ VI, IuV C, Fomkina MG, Montrel MM. A potentiometric sensor designed on the basis of urease immobilized in polyelectrolyte microcapsules. Biofizika. 2007; 52: 825-829.